Science of the Total Environment 407 (2009) 4986–4993

Contents lists available at ScienceDirect

Science of the Total Environment

journal homepage: www.elsevier.com/locate/scitotenv

Evaluation of nanoscale zerovalent iron particles for trichloroethene degradation in clayey soils

Yelena P. Katsenovich *, Fernando R. Miralles-Wilhelm

Applied Research Center, Florida International University, 10555 W. Flagler St., Suite 2100, Miami, FL, 33174, United States

ARTICLE INFO

Article history:
Received 20 September 2008
Received in revised form 11 April 2009
Accepted 21 May 2009
Available online 30 June 2009

Keywords:
Nanoscale zerovalent iron
Palladized bimetallic particles
Deactivation rate constant
Dechlorination
Agglomeration

ABSTRACT

The longevity and reactivity of nanoscale zerovalent iron (nZVI) and palladized bimetallic particles (BNP) were evaluated in batch and column experiments for remediation of a trichloroethene (TCE)-contaminated plume within a clayey soil from Oak Ridge Reservation (ORR). Comparative studies assessing the viability of BNP and nZVI confirmed that particle behavior is severely affected by clay sediments. Surface morphology and composition analyses using SEM and SEM–energy-dispersive spectroscopy spectrum revealed particle agglomeration through the formation of clay–iron aggregates of greater mass during the early phase of the experiment. Batch study results suggest that TCE degradation in ORR clayey soil follows a pseudo-first-order kinetic model exhibiting reaction rate constants (k) of 0.05–0.24 day^{-1} at varied iron-to-soil ratios. Despite high reactivity in water, BNP were less effective in the site-derived clay sediment with calculated TCE removal efficiencies of 98.7% and 19.59%, respectively.

A column experiment was conducted to investigate particle longevity and indicator parameters of the TCE degradation process under flow conditions. It revealed that the TCE removal efficiency gradually declined over the course of the experiment from 86–93% to 51–52%, correlating to a progressive increase in oxidation–reduction potential (ORP) from −485 to −250 mV and pH drop from 8.2–8.6 to 7.4–7.5. The rate of nZVI deactivation reaction was found to be a first order with a k_d value of 0.0058 day^{-1}. SEM images of residual nZVI revealed heavily agglomerated particles. However, despite widespread oxidation and agglomeration, particles managed to maintain some capacity for oxidation. A quantitative analysis of nZVI deactivation has the potential of predicting nZVI longevity in order to improve the design strategy of TCE remediation.

Published by Elsevier B.V.

1. Introduction

Soil and groundwater contamination by trichloroethylene (TCE), as well as other chlorinated ethenes has proved interminably persistent, warranting a massive search for effective mitigative strategies that has resulted in a number of possibilities. Of these, treatment methods incorporating granular zero-valent iron (ZVI) and nanoscale ZVI (nZVI) have emerged as amongst the most promising. Both methods have been shown to dechlorinate TCE via a reductive surface-mediated process, a consequence of the direct oxidative corrosion of Fe to Fe(II) (Matheson and Tratnyek, 1994; Orth and Gillham, 1996; Arnold and Roberts, 2000). The proposed reaction pathways for TCE degradation are β-elimination (primary), hydrogenation (minor) and hydrogenolysis (minor). The first two mechanisms explain the formation of ethene and ethane, while a minor portion of TCE decomposed by the third can result in the formation of *cis*-dichloroethene (DCE) and vinyl chloride (VC) (Roberts et al., 1996; Su and Puls, 1999; Liu et al., 2005).

Previous studies have demonstrated that reducing conventional ZVI particle size to 10–100 nm increases surface area and reactivity and potentially simplifies delivery via injection to contaminated zones located well below the ground surface (Wang and Zhang, 1997; Choe et al., 2001; US EPA, 2005). nZVI can be synthesized via the borohydride-catalyzed reduction of dissolved Fe(II) or Fe(III) (Zhang, 2003). Wang and Zhang showed that freshly synthesized nZVI exhibits a significantly greater surface reactivity than commercial iron powders (Wang and Zhang, 1997). In several studies, the effect of nZVI has been enhanced via complexation of the iron with Pd (Pd/nZVI) (Lien and Zhang, 2001).

The Oak Ridge Reservation (ORR), a site in Tennessee known to encompass a number of areas in which there is substantial subsurface contamination by chlorinated ethenes such as perchloroethene (PCE) and TCE was chosen as the primary study site for this investigation. In particular, a TCE-contaminated plume was detected about 21 to 24 m below ground surface within a fractured bedrock aquifer of the Oak Ridge National Laboratory (ORNL) 7000 Area. TCE concentrations in groundwater near the suspected source are on the order of 10 mg L^{-1}.

The composition of the bedrock lining the boundaries has revealed its predominant components primarily consist of low in organic carbon illite, quartz, calcite, kaolinite, and plagioclase feldspar. Its sand–silt–clay distribution (wt.%) has been defined as 30.8–50.4–18.8 (Watson et al., 2004). Han et al. (2006) reported higher clay content

* Corresponding author. Tel.: +1 305 348 2338; fax: +1 305 348 5018.
E-mail address: katsenov@fiu.edu (Y.P. Katsenovich).

0048-9697/$ – see front matter. Published by Elsevier B.V.
doi:10.1016/j.scitotenv.2009.05.033

with the corresponding distribution of 22–41–37 in ORR soil. Both results correspond to prior characterizations of clayey soil (Cetin, 2004; Cetin et al., 2006).

A preliminary assessment of the geological baseline parameters revealed negative results for *Dehalococcoides ethenogenes* (DHC) bacteria DNA analyses performed on site-derived soil and groundwater confirming that existing environmental conditions at ORR were not favorable to anaerobic reductive dechlorination bacteria. These findings, coupled with an insufficient capacity for natural attenuation contribute to the persistence of TCE contamination in this area. The plume depth, its proximity to the point of groundwater discharge, and the fractured bedrock environment have underscored the importance of finding an effective technology for TCE remediation in the ORNL area. Several studies have investigated the reactivity of nZVI with chlorinated organic compounds in the presence of clay fines (kaolin) (Reddy and Karri, 2008; Kim et al., 2008); however, no results have been reported on the performance of nZVI in soils collected from the contaminated site.

The main objectives of this study were to evaluate the efficiency of nZVI in bench and in continuous-flow column systems and compare the use of nZVI and modified BNP for the remediation of chlorinated solvents in clayey soil. A unique set of environmental conditions endemic to the study site was replicated to the extent possible in all tests.

2. Experimental section

2.1. Materials

TCE stock solutions were prepared using certified A.C.S. grade TCE (99+%, Fisher Scientific) according to US EPA Method 624. Neat standard grade 1,1-DCE, *trans*-1,2-DCE, *cis*-1,2-DCE and VC were used for analytical standard preparations (Supelco-Bellefonte, PA). Batch tests and column experiments were conducted using deoxygenated reverse osmosis (RO) pretreated tap water (Barnstead International). The use of a consistent aqueous medium in all tests enabled us to establish baseline parameters and to characterize the effect of site-derived clayey soil on nZVI reactivity and agglomeration. Deoxygenated water (DOW) was produced by purging RO with nitrogen for 2 h and was subsequently stored in an anaerobic chamber (Coy Laboratory Products Inc.) containing an atmosphere of 95% N_2 and 5% H_2. All batch reactor preparations such as DOW distribution and particle weighing and distribution, were performed under anaerobic conditions. Deoxygenated deionized water (DODW), prepared by purging deionized water with nitrogen for 2 h was used in the synthesis of nZVI and BNP.

Contaminated site-derived soil dominated by clay- and silt-sized particles was air-dried at room temperature, ground and passed through a 2 mm sieve. Prior to the start of the experiment, soil weight was stabilized by drying at 75 °C and cooling in a desiccator to facilitate precise weight measurements. Analysis of a representative set of processed samples revealed values of 1.227 g cm^{-3}, 2.655 g cm^{-3} and 0.54 for dry bulk density, particle density and porosity, respectively.

Sodium borohydride ($NaBH_4$, 98%), ferric chloride ($FeCl_3 \cdot 6H_20$, 98%) and palladium acetate ($[Pd(C_2H_30_2)_2]_3$, 99%, Acros Organics) were purchased from Fisher Scientific. Calibration gas for the GC/FID, a standard mixture containing 15 ppm each methane, ethane, ethene, ethyne, propane and propene and balanced with nitrogen gas, was obtained from Matheson, Tri-Gas, (Micro Mat 14) Alltech, IL. Commercial nZVI (average particle size — 120 nm, 99% purity, surface area 4–6 m^2/g, Argonide Corporation, Sanford, FL) was obtained from Fisher Scientific. All solutions used for nZVI synthesis were prepared with DODW.

Ferrous iron analyses chemicals: hydroxylamine hydrochloride ($NH_2OH \cdot HCl$, 99%), ammonium acetate ($NH_4C_2H_3O_2$, 99%), sodium acetate ($NaC_2H_3O_2 \cdot 3H_2O$), phenanthroline ($C_{12}H_8N_2 \cdot H_2O$, 99%), ferrous sulfate heptahydrate ($FeSO_4 \cdot 7H_2O$, Certified ACS) and diisopropyl ether ($C_6H_{14}O$, 99%) were purchased from Fisher Scientific.

2.2. Experimental procedures

2.2.1. Particle preparation

nZVI particles were prepared using the solution method described by Zhang (2003). Synthesized particles were recovered by vacuum-filtration using a Durapore membrane (0.45 μm) and, where appropriate, were subsequently used for the BNP preparation. Palladized particles were prepared by a method of reductive deposition (Grittini et al., 1995; Zhang et al., 1998). Wet, vacuum-filtered iron particles were coated with a thin layer of Pd by saturating them in a methanol solution containing 1% wt (0.1% w/w Fe) $[Pd(C_2H_3O_2)_2]_3$. Fresh particles were recovered by vacuum filtration, washed with excess DODW, rinsed in ethanol and then recovered by vacuum filtration once more before use in experimental batches. The size range and surface area of BNP synthesized by this method were determined to be 1–100 nm and 33.5 m^2/g, respectively (Zhang et al., 1998).

2.2.2. Commercial nZVI and BNP reactors

All batch tests were conducted in 250 mL serum bottles tightly capped with Teflon Mininert valves. Reactors contained 50 g of processed soil, 150 ml DOW, and a specific mass of nZVI particles resulting in a soil/solution mass ratio of 0.3. Three sets of batch reactors containing commercial nZVI were prepared to examine iron-to-soil ratios of 0.001, 0.0025, and 0.004, in the treatment of a targeted concentration of 8–10 mg L^{-1} TCE. 100 μL of 113.688 mM (14,950 ppm) TCE stock solution was spiked to soil suspensions and controls. Supplemental control reactors containing only DOW were set up in triplicate to determine the exact mass of TCE injected to all batch reactors (Table 1). A parallel no-soil control set was used to determine the effect of clayey soil on TCE degradation. 200 mg nZVI was injected to a DOW suspension, making this set analogous to an iron-to-soil ratio of 0.004. Sets comprised of 11–13 identical sacrificial reactors, each of which were sampled at different time intervals and immediately discarded. These reactors were the primary source of pH and oxidation–reduction potential (ORP) readings and microstructure

Table 1
Evaluation of commercial and Pd/nZVI particles.

Particle type	Iron/soil	Initial TCE (μm)	Final VOC (μm)	VOC reduction (%)	*cis*-DCE in suspension (ppm)	Final pH	Average ORP (mV)	k (day^{-1})	R^2
Commercial	0.001	16.143 ± 0.23	12.18	24.5	0.021 ± 0.01	7.75–7.8	−276 ± 32	0.023	0.73
	0.0025	16.43 ± 0.056	11.05	32.8	0.03 ± 0.009	7.7–8.2	−344.6 ± 27	0.052	0.83
	0.004	16.43 ± 0.056	4.83	70.6	0.054 ± 0.01	8.05–8.14	−420 ± 54	0.107	0.83
	0.024	15.928 ± 1.39	0.45	97.2	0.041 ± 0.025	8.8–8.9	−387 ± 28	0.151	0.99
	0.036	15.928 ± 1.39	0.09	99.4	0.052 ± 0.035	9.04–9.06	−467	0.213	0.93
	0.004[a]	16.43 ± 0.056	0.091	99.4	ND	8.2	−400	0.238	0.998
BNP	0.0056	11.155 ± 0.466	8.97	19.6	ND	7.5–7.89	−347 ± 20	0.869	0.91
	0.0056[b]	11.155 ± 0.466	0.14	98.7	ND	7.15–7.25	−669 ± 36	2.226	1

[a] No-soil control with addition of 200 mg nZVI.
[b] No-soil control with addition of 280 mg BNP.

analyses. Likewise, a sacrificial set and a parallel no-soil control were prepared to evaluate BNP at an iron-to-soil ratio of 0.0056.

Reactors prepared in duplicate and containing commercial iron-to-soil ratios of 0.024 and 0.036 were used to determine the concentrations of TCE and byproducts over time. Each duplicate reactor was non-destructively analyzed multiple times over a set experimental period.

The masses of TCE chlorinated intermediates in the reactors were determined according to the dimensionless Henry's Law constants at 20 °C [0.314(TCE), 0.140(*cis*-1,2-DCE), 0.359(*trans*-1,2-DCE), 0.975(1,1-DCE), 0.891(VC)] (Gossett, 1987; Staudinger and Roberts, 2001). Control reactor headspace was calculated to be 100 mL while that of the experimental reactors were found to be about 82.4 mL after considering sediment volume. All reactors were shaken manually several times per day.

In addition, assessment of TCE adsorption onto soil was conducted in triplicate batch reactors without a head space using identical TCE concentrations and soil/solution ratio to the experimental reactors. The TCE sorption partitioning coefficient K_d value was estimated at 0.53 ± 0.09 mL g^{-1}.

2.2.3. Column preparation

Two continuous-flow column systems were set up to study the effect of commercial nZVI on TCE degradation in clayey soil. The Pyrex glass columns used were 5 cm in diameter and 45 cm long with stainless steel end caps. Stainless steel was found to be the least reactive metal in the reduction of halogenated compounds due to it inertness with respect to corrosion (Alonso et al., 2002). Each was equipped with four equally spaced sample ports. Glass wool covered the inlet fitting and the inner side of the sampling tubes to minimize clogging. The control column was assembled without added iron and packed with site-derived soil while the experimental column was set up with an iron-to-soil ratio of 0.007. Soil was crushed into small aggregates, mixed with the commercial nZVI in 200 g increments and packed into the column. The dry weights of soil in the control and experimental columns were 800 g and 870 g, respectively. Initial porosity approximated 50% as per results derived during the preliminary characterization.

The column reactors were continuously fed DOW with approximately 8.20 ± 2.13 mg L^{-1} ($63.12\ \mu mol \pm 16.20 \mu mol$) TCE in the inlet solution. This was pumped into the column in an up-flow mode at a volumetric flow rate (v_0) of 0.336 ± 4.7 L day^{-1}, resulting in a fluid velocity of 0.059 cm min^{-1} and a hydraulic retention time of approximately 1.1–1.2 days, dependent upon soil porosity and volume. The feed solution was prepared twice per week and stored in a 5-millimeter thick Teflon bag that contained no headspace to eliminate the possibility of TCE partitioning into the gas phase. ORP and pH were regularly monitored at each sampling port using the pH/ORP Controller (Eutech Instruments) fitted within a flow-thru micro cell. The microelectrodes used (Microelectrodes, Inc.) allowed measurements to be taken with 1.5 to 2 mm of electrode immersion. Following pH/ORP determination, liquid samples were kept in flow-thru 40-mL vials for GC/MS analyses. Upon completion of column experiments, magnet-extracted residual iron particles were thoroughly washed several times with methanol to remove remaining soil fines from the surface and then exploited via microstructure analysis.

In addition, the control column was used to measure the TCE adsorption onto soil. The adsorption of TCE was calculated from the experimental breakthrough curve once a 50% breakthrough was achieved. The distribution coefficient, K_d, was determined at the moment when the relative concentration calculated as a ratio of effluent and influent concentrations became equal to 0.5 as follows:

$$K_d = (R - 1)\theta / \rho \quad (1)$$

where ρ is the soil bulk density and θ is the volumetric water content. The retardation factor, R, is the number of pore volumes at which the relative concentration of the observed breakthrough curve reaches a value of 0.5 (Van Genuchten and Wierenga, 2003). Fifty percent of TCE breakthrough occurred within 2 pore volumes that resulted in a K_d value of 0.44 mLg^{-1}. The column derived K_d agreed favorably with the K_d determined in the batch experiments.

2.2.4. Analytical procedures

Ethyne, ethene, and ethane analysis were conducted using a PerkinElmer Clarus 500 GC (column: Carboxen 1006 Plot Capillary (Supelco 30 m × 0.53 mm); detector: FID; LOD targeted analytes: ≤20 ppb). The instrument was calibrated prior to any analyses by comparing retention times and peak areas with standard commercial gas mixture samples.

Liquid sampling occurred after the full precipitation of solids. In sacrificial sets the supernatant was transferred through a 3 mm glass tube to a 40 mL analytical vial by applying positive pressure of injected nitrogen to the reactor. Sampling in duplicate batches was conducted by extracting 1–5 mL of the supernatant using a gas-tight syringe. Dilution factors were obtained by injecting this liquid slowly into a 40 mL analytical vial containing a known volume of DODW. All vials were acidified, tightly sealed, and analyzed via GC/MS.

Aqueous concentrations of TCE and the chlorinated byproducts of its degradation were determined simultaneously by the SW-846 purge and trap GC/MS method using sample preparation method EPA 5030B and analytical method EPA 8260B. The analyses were performed on a Varian Star 3400cx GC/Varian Saturn 2000 MS coupled with a Tekmar Dohrmann 3100 sample concentrator (TCE, DCE and VC LOD: 3 μg L^{-1}, 3 μg L^{-1}, and 2 μg L^{-1}, respectively). Samples were introduced to the concentrator using an Archon purge and trap auto sampler with 5 mL injection volume from the 40 mL glass vials. Ultrahigh-purity helium gas and fluorobenzene were used as the carrier gas and internal standard, respectively. QC samples (QCS) were prepared using VOC check solutions for two different concentration points in each run. These check solutions were only used to prepare the QCSs. Reproducibility of the liquid-phase analysis was checked in each run twice by analyzing TCE standard solutions.

Ferrous iron analyses were conducted according to the Phenanthroline Method (method No. 3500-Fe-D) and collected samples were analyzed using a UV-1601 UV/VIS Shimadzu Spectrophotometer (APHA, 1995).

In sacrificial sets, the release of soluble iron into solution and changes in pH and ORP were measured from the remaining water suspension after sample extraction. The ORP probe was a combination electrode and all values reported are electrode potentials with respect to Ag/AgCl reference. Residual particles were extracted with a magnetic rod after sample collection, pH and ORP measurements, washed with DODW and methanol, and kept in a methanol solution in the anaerobic chamber until microstructure analysis, which was done with a JOEL, JSM-6330F SEM at 15 kV. Particle composition was analyzed using a SEM–Energy-Dispersive-Spectrometry (SEM–EDS) Noran System Six Model 200.

3. Results and discussion

3.1. Reactivity of nZVI

As shown in Fig. 1, increases in the iron-to-soil ratio were correlated with the enhanced reductive dechlorination of TCE. However, efficiency of VOC mass removal was not directly proportional to increased iron concentration. The increase in the ratio from 0.001 to 0.0025 did not appear to contribute to VOC reduction, while another increase from 0.004 to 0.036 increased TCE removal from 55.6% to 99.45%. Although all chlorinated by-products of TCE degradation were quantitatively analyzed at each sampling event, only *cis*-1,2-DCE was identified in the liquid suspension. Concentrations of this compound fell within the

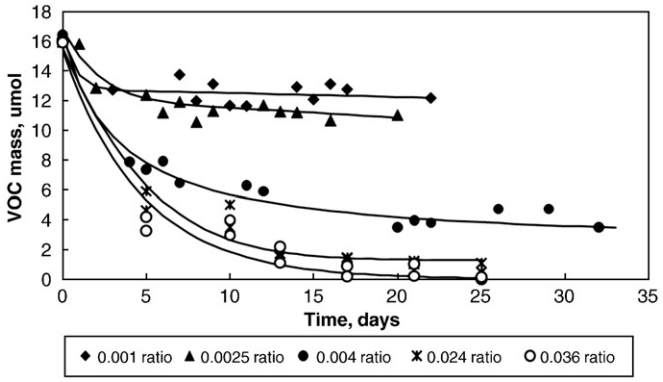

Fig. 1. VOC mass reduction in commercial nZVI reactors over time at various iron-to-soil ratios.

range of 0.021 ± 0.01 to 0.054 ± 0.01 ppm in the experimental reactors (Table 1).

For the 20–35 days over which each experiment was conducted, the concentration of Fe (II) in the reactor suspensions increased from non-detectable levels to 3.0–6.1 ppm in proportion to the amount of nZVI added. pH values were seen to increase from an initial 7.0–7.2 to a maximal range of 9.04–9.06, while ORP was lowered to a range of −276 to −467 mV; in some cases to as low as −503 mV. These results suggest that iron-to-soil ratios greater than or equal to 0.0025 are needed to create the reductive conditions (ORP < −300 to −500 mV) suitable for abiotic reduction (beta-elimination) of TCE (Table 1). Gavaskar et al. (2005) reported that the 0.004 iron-to-soil ratio in the treatment zone was enough to create a sufficient reductive environment for the abiotic degradation of TCE; however, they recommended the use of excess iron mass to account for possible consumptions and passivation by native oxidized species in the groundwater.

Control reactors showed 99.45% reduction — much higher than that observed in analogous soil-containing reactors (Table 1). Additionally, no chlorinated byproducts were identified, suggesting that the clay soil used in the sample reactors has affected nZVI reactivity. TCE concentrations in the controls declined sharply for the first 5–6 days before reaching a steady state with no further degradation. Similar behavior was observed by Lee and Batchelor (2002a, 2002b) in suspensions of iron-bearing minerals in which TCE concentrations were rapidly reduced in the initial phase and then slowly declined before reaching a steady state.

The following first order reaction kinetic equation was used to describe concentration–time measurements in batch reactors:

$$-dC/dt = -r_A = kC. \quad (2)$$

VOC concentration (μmol L^{-1}) at any time is given by:

$$C = C_0 e^{-kt} \quad (3)$$

where C and C_0 are TCE concentration (μmol L^{-1}) at time t (day) and at time $t = 0$, respectively; k is the specific rate constant, r_A is the reaction rate (Fogler, 1998). Rate coefficients were determined with 95% confidence via nonlinear regression analyses using MATLAB software. The resulting curves were best fitted to exponential equations with computed reaction rate k constants listed in Table 1. With regard to the commercial iron sets, the increase of iron-to-soil ratios is correlated with the increase of rate constants and 0.036 ratio gave the highest k value (0.213 day^{-1}), resulting in 99.45% TCE mass removal. This k value is comparable to the rate coefficient of 0.238 day^{-1} for the no-soil control.

Qualitative analyses of the non-chlorinated C_2 byproducts of TCE reduction were conducted prior to each liquid sampling. Ethyne, ethene and ethane were detected in the headspace of all nZVI-treated, TCE-spiked soil reactors in a distribution of 4.66% ± 4.7, 61.7% ± 10.2 and 34.6% ± 9.51, respectively. Only ethene and ethane were observed in parallel TCE-spiked control reactors. Ethyne was not produced in the absence of iron. These observations are consistent with the proposed pathways for TCE dechlorination; reductive elimination (TCE → chloroethyne → ethyne → ethene), hydrogenolysis (TCE → *cis*-DCE → VC → ethene) and hydrogenation (ethene → ethane) (Roberts et al., 1996; Liu et al., 2005).

3.2. Evaluation of BNP

Like commercial nZVI, palladized particles elicited greater degradation in DODW than soil; however, the site-derived clay sediment seemed to affect BNP much more than the former (Fig. 2a). TCE removal in the control and experimental reactors was calculated to be 98.7% and 19.59%, respectively. This data is correlated with an increase in soluble Fe (II) in the control and experimental reactors from non-detectable to 9.7–11 and 1.4–2.8 ppm, respectively. BNP reacted quicker with a degradation rate of 0.869 day^{-1} compared to a nZVI rate of 0.107–0.151 day^{-1} determined for ratios 0.004–0.024 but was spent more rapidly (Table 1). It is important to note that BNP are less effective if silt or dense clay is present in the underlying geology. Chlorinated byproducts were not detected in either control or experimental suspensions at the close of the experiment. As in previous studies, only ethene and ethane (no ethyne) were detected in the headspace (Choe et al., 2001).

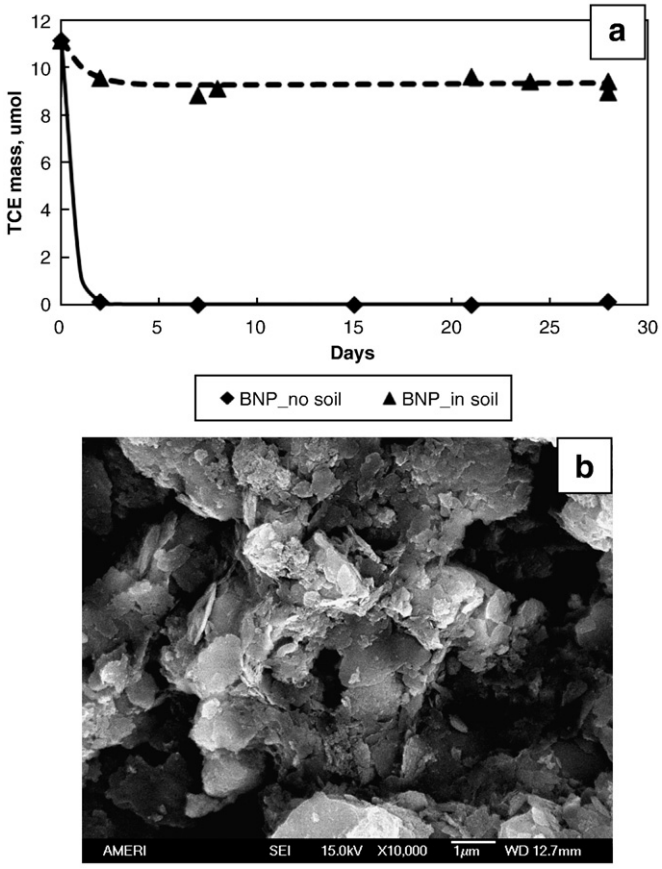

Fig. 2. (a) BNP (Pd) Performance); (b) SEM image of BNP residual particles after completion of experiment.

3.3. Microstructure analyses

The morphology and microstructure of commercial particles are shown in Fig. 3. Initially, particle diameters ranged from 40 and 100 nm with some larger particles approaching 1 μm. As determined by SEM images, particle agglomerated during the experiment with the size between 10 and 50 μm. This observation correlates with Phenrat et al. (2007) conclusions that magnetic attractive forces between nZVI affect their dispersive stability in aqueous solutions with the result that particles 20 nm in diameter aggregated to form micrometer-sized clusters. The detection of soil-derived Al (%) and Si (%) on the oxide shell surface by SEM–EDS (Fig. 3) confirmed that the attachment of nZVI to clay fines resulted in iron particles agglomeration through the formation of clay–iron aggregates of greater mass. The presence of the oxygen peak on the SEM–EDS images with 5.14%–25.92% weight is the evidence of the oxide magnetite (Fe_3O_4) and maghemite (Fe_2O_3) shell formation at the Fe^0/Fe-oxide interface (Kohn et al., 2005; Liu and Lowry, 2006). Magnetite and maghemite were the only oxide phases found in crystalline nZVI particles (Toda Kogyo Corp., Japan) before and after exposure to H_2O or TCE/H_2O solutions (Nurmi et al., 2005). This is consistent with the observed reduction in nZVI reactivity during the course of the experiment. On the other hand, despite the occurrence of a certain amount of corrosion, partial oxidation of particles was not observed to cease completely.

Pd/nZVI, having the surface coating catalyst, was more reactive in aqueous solutions showing rapid destruction of TCE. Alternately, in clayey soil BNP become oxidized much faster and to a greater degree than do commercial nZVI. It is likely that the formation of clay–iron aggregates in a manner analogous to commercial nZVI reduces particle reactivity. As determined by SEM–EDS analyses of residual BNP, the percentage of oxygen component was found to increase by up to 60% suggesting that iron is primarily present in the oxide form. The weight percent of soil-derived Al and Si were determined in the range of 8.11%–11.8% and 16.98%–28.44% which is much higher than the corresponding values obtained for the commercial nZVI (images not shown). While the iron core still exists, its reactivity is completely inhibited by this oxide coating and the formation of clay–iron aggregates. This observation is supported by a number of earlier field studies (US EPA, 2005). Pd/nZVI becomes oxidized much faster and to a greater degree than do commercial nZVI, helping to explain why BNP are more reactive in aqueous solutions, but subjected to faster oxidation and agglomeration in clay (Fig. 2).

Of all the nZVI types analyzed in the batch experiments, only commercial particles showed prolonged reactivity in terms of TCE removal, an observation further substantiated by microstructure analyses (Lien and Zhang, 2001). Additional investigations must be conducted to evaluate effective means of overcoming nZVI agglomeration in order to increase the practical viability of these particles *in situ*.

3.4. The column experiment

The aggregation aspects of nZVI particles have been studied by several researchers (Liu et al., 2005; Phenrat et al., 2007). Kim et al. (2008) noted that the presence of clay fines (2 to 15%) in water saturated sand columns greatly reduced the nZVI mobility at pH 8 and reported the attachment of modified nZVI to kaolinite at pH<8. However, the longevity of particles in continuous flow systems has not been evaluated yet. The purpose of the column experiment was to determine particle longevity, indicator parameters of the process, the nZVI first-order deactivation constant k_d, and a decline in the percent of TCE removal under flow conditions mimicking those found at ORR. The decision to use commercial particles for the column experiment was influenced by the relatively fast oxidation and greater agglomeration tendencies of BNP, coupled with the observed in batch experiments inefficiency of the latter in clayey environments.

During the 127 days over which the experiment was conducted, TCE effluent concentration increased from 0.5 to 3.3 mg L^{-1}, reflecting the progressive decrease in TCE removal from 86–93% to 51–52% and increase in the molar rate at which TCE left the column from 1.17–2.52 to 9.15 μmol day^{-1}. This takes into account both TCE influent (C_{A0}) (μmol L^{-1}) and effluent (C_A) (μmol L^{-1}) concentrations at time t, and the entering volumetric flow rate (v_0) (L day^{-1}).

The nZVI deactivation constant for the TCE degradation reactions was determined using separable kinetics, which define decreasing nZVI activity (a) at time t as the ratio of the rate of reaction (r_A) at t to the initial reaction rate (Fogler, 1998).

$$a(t) = \frac{-r_A(t)}{-r_A'(t=0)}. \tag{4}$$

The mole balance for reaction is

$$v_0 \frac{dC_A}{dW} = -ka(t)C_A. \tag{5}$$

Solving for the activity, $a(t)$ results in:

$$a(t) = \frac{v_0}{Wk} \mathrm{Ln} \frac{C_{A0}}{C_A}. \tag{6}$$

The plot of [$\mathrm{Ln}C_{A0}/C_A$)] versus t results in a line with a slope equivalent to the nZVI deactivation rate constant k_d (0.0058 day^{-1}) (Fig. 4b) (Fogler, 1998).

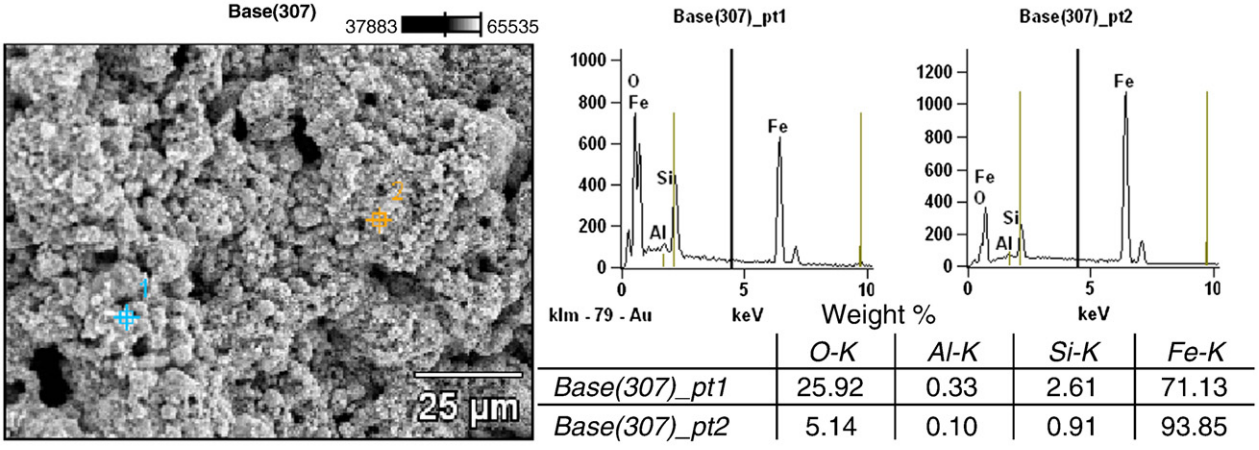

Weight %

	O-K	Al-K	Si-K	Fe-K
Base(307)_pt1	25.92	0.33	2.61	71.13
Base(307)_pt2	5.14	0.10	0.91	93.85

Fig. 3. SEM–EDS composition for residual commercial particles 10 days after the beginning of the experiment (magnification: 1000).

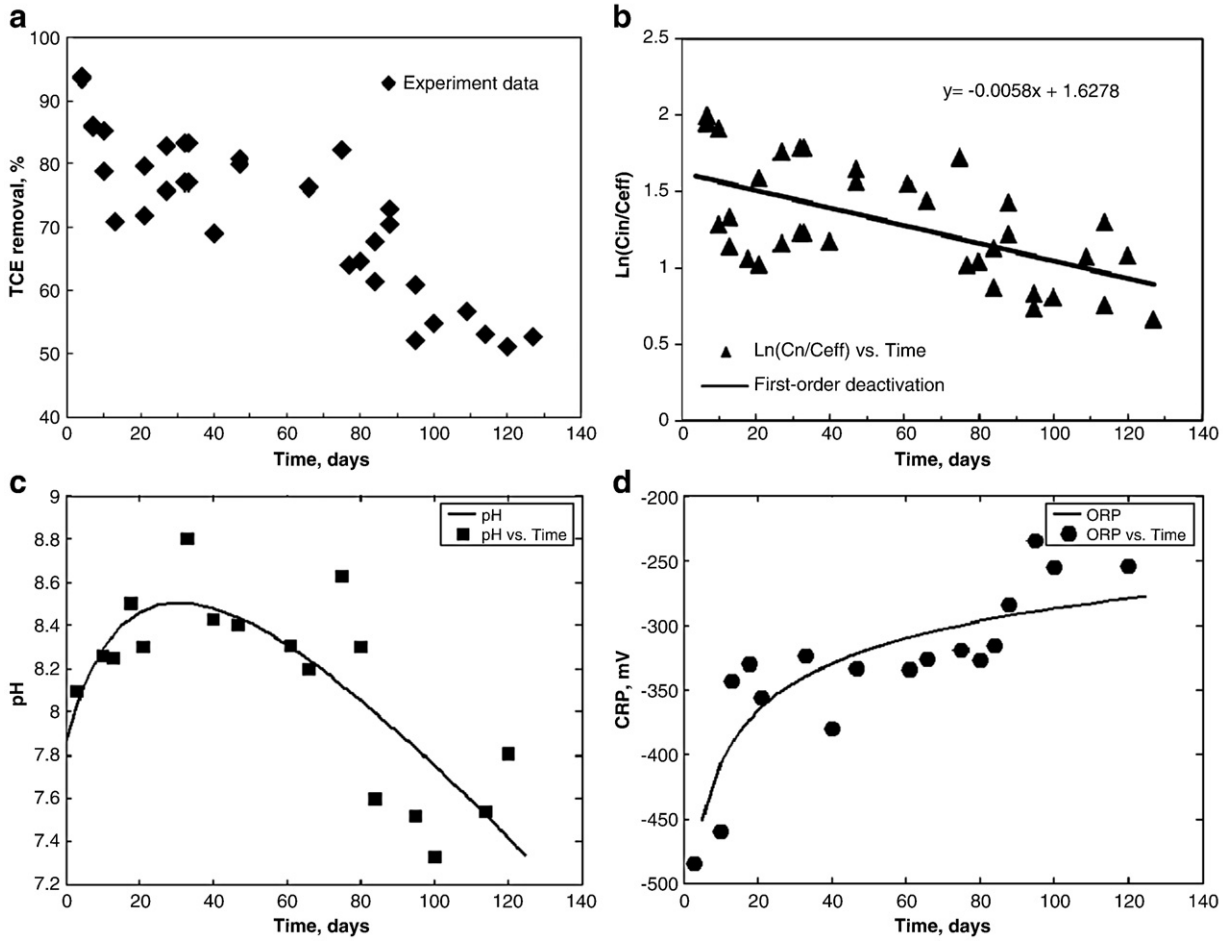

Fig. 4. a) Decline in percent removal of TCE; b) First-order deactivation constant, c) Experimental column — pH of interstitial water, d) Experimental column — ORP of interstitial water.

The loss of nZVI activity due to nanoparticles oxidation and agglomeration follows first-order reaction, which was applied to model nZVI deactivation. First-order deactivation is given by:

$$a(t) = e^{-k_d t} \tag{7}$$

Calculations show that nZVI for the duration of the column experiment has deactivated to the extent that its activity was only 48% compared to the initial. Decline in nZVI activity agreed well with the decrease in the percentage of TCE removal (51%) observed in the column experiments (Fig. 4a). The loss of nZVI activity can be modeled by the first-order reactions to estimate its activity at time *t*. A quantitative analysis of deactivation law has the potential of predicting nZVI longevity in order to improve the design strategy of TCE remediation.

Interstitial water in the control column maintained pH and ORP values in the range of 6.8–7.2 and −130 to −180 mV, respectively. After soil was fully saturated and TCE adsorption was complete, the

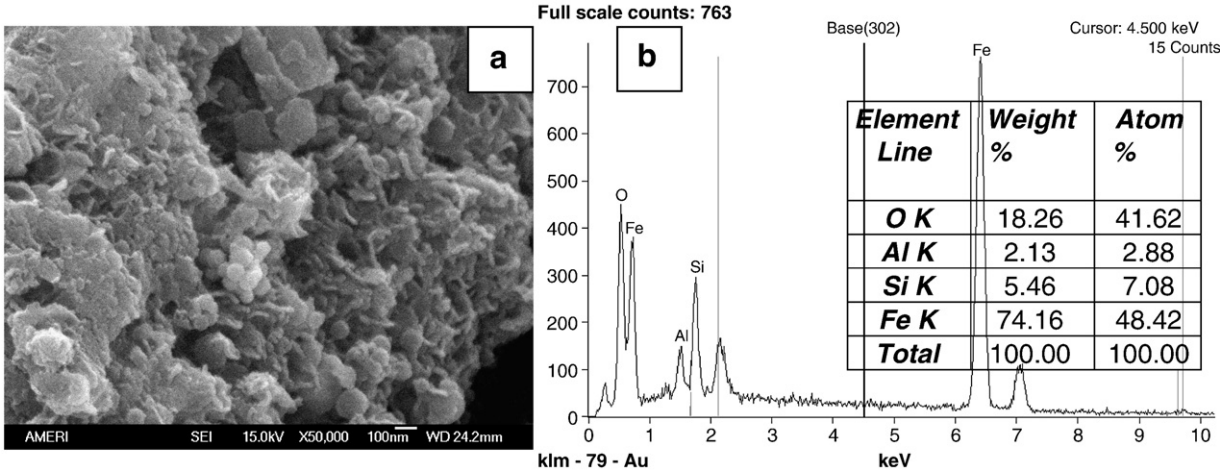

Fig. 5. (a) SEM images of residual commercial particles after the completion of the column experiment. (b) SEM–EDS for residual column particles.

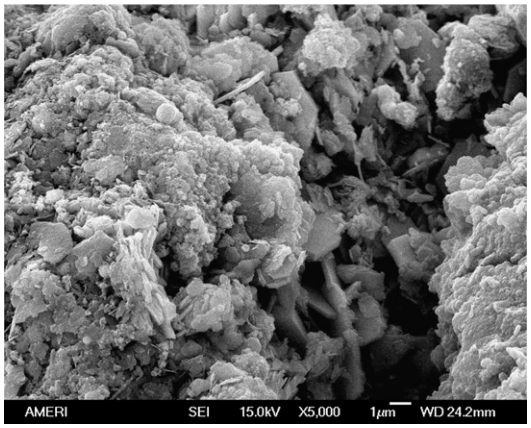

Fig. 6. SEM images of residual commercial particles after the completion of the column experiment. Magnification: 5000.

effluent TCE concentration was roughly the same as the influent and no chlorinated intermediates were observed (data is not shown).

The ORP of interstitial water in the experimental column gradually increased from −485 to −250 mV (Fig. 4d), while pH declined from 8.2–8.6 to 7.4–7.5 (Fig. 4c). ORP remained conducive to TCE abiotic degradation over the better half of the experiment (~80 days). As nZVI reactivity dropped, this correlated with an increase in ORP to non-conducive values. These results are much lower than those when iron was first introduced into the system, but still higher than that of the control column.

An SEM image of magnet-extracted particles is shown in Fig. 5. These images, coupled with the SEM–EDS spectrum strongly suggest the occurrence of advanced oxidation and agglomeration after 127 days of experimental conditions. Additionally, a much higher weight percent of O, Al and Si were detected on the oxide shell surface than had been identified in batch-extracted particles. The weight percent of Al and Si in turn increased up to 2.13%, and 5.46% compare to the batch detected values (Fig. 3). SEM images of residual nZVI revealed heavily agglomerated particles. The size of aggregates was determined to be in the 10–100 μm range (Fig. 6) compared to the initial 40–100 nm. However, despite widespread oxidation and agglomeration, particles managed to maintain some capacity for oxidation.

The corrosion of nZVI resulting in the formation of the oxide shell decreases its reactivity with the target contaminant. This entails additional nZVI injections to sustain reducing conditions necessary for the abiotic reduction of TCE. Furthermore, the presence of clay minerals results in nZVI agglomeration and creation of clay–iron aggregates with the size range of 10–100 μm. This may substantially limit particles mobility and their effective distribution in subsurface. These factors should be carefully considered in designing remediation strategies for clayey soils.

Acknowledgements

Funding for this research was provided by US DOE Grant Number: E-FG01-05EW07033. We would like to acknowledge Dr. Yanqing Liu from the FIU Mechanical Engineering Department for his assistance with the SEM images and the nZVI microstructure analysis. We would also like to thank Richard Ketelle of Bechtel-Jacobs for providing us with sample materials and information related to the ORNL 7000 Area study site and Sirem Company (Canada) for assistance in assessing baseline parameters at ORR.

Appendix A

Abbreviations

BNP	palladized bimetallic particles
DCE	dichloroethene
DOW	Deoxygenated water
DODW	Deoxygenated deionized water
DHC	*Dehalococcoides ethenogenes*
DIW	deionized water
nZVI	Nanoscale ZVI
ORP	oxidation–reduction potential
ORR	Oak Ridge Reservation
PCE	perchloroethene
Pd/nZVI	palladized nZVI
RO	reverse osmosis
SEM–EDS	SEM–energy-dispersive spectroscopy spectrum
TCE	trichloroethene
US DOE	U.S. Department of Energy
VC	vinyl chloride
VOC	volatile organic compound

Symbols

Batch Reactors

C	TCE concentration (μmol L^{-}) at time t
C_o	TCE concentration (μmol L^{-1}) at time $t=0$
k	specific reaction rate constant
k_1	Calculated reaction rate constants
r_A	reaction rate
t	time

Columns

a	nZVI activity
C_{A0}	TCE influent (μmol L^{-1})
C_A	TCE effluent (μmol L^{-1})
F_{A0}	$v_0\ C_{A0}$ = TCE molar flow rate (μmol day^{-1}) into the system
F_A	$v_0\ C_A$ = TCE molar flow rate (μmol day^{-1}) out of the system
k_d	deactivation rate constant (day^{-1})
n	reaction order
r_A	reaction rate
t	time (day)
v_0	volumetric flow rate (L day^{-1})
W	nZVI mass (g) in column

References

Alonso F, Beletskaya IP, Yus M. Metal-mediated reductive hydrodehalogenation of organic halides. Chem Rev 2002;102(11):4009–92.
American Public Health Association (APHA). Standard Methods. 19th Ed. Washington, DC: APHA; 1995.
Arnold WA, Roberts AL. Pathway and kinetics of chlorinated ethylene and chlorinated acetylene reaction with Fe(0) particles. Environ Sci Technol 2000;34:1794–805.
Cetin H. Soil-particle and pore orientations during consolidation of cohesive soils. Eng Geol 2004;73:1-11.
Cetin H, Fener M, Gunaydin O. Geotechnical properties of tire-cohesive clayey soil mixtures as a fill mixture. Eng Geol 2006;88:110–20.
Choe S, Lee S-H, Chang Y-Y, Hwang K-Y, Khim J. Rapid reductive destruction of hazardous organic compounds by nanoscale Fe^0. Chemosphere 2001;42:367–72.
Fogler HS. Elements of Chemical Reaction Engineering. 3rd Ed. Upper Saddle River: Prentice Hall PTR; 1998.
Gavaskar A, Tatar L, Condit W. Nanoscale zero-valent iron technologies for source remediation. Cost and performance report. Prepared for Naval Facilities Engineering Service Center under the contract number N47408-01-D-8207; 2005.
Gossett JM. Measurement of Henry's Law Constant for C_1 and C_2 chlorinated hydrocarbons. Environ Sci Technol 1987;21:202–8.
Grittini C, Malcomson M, Fernando Q, Korte N. Rapid dechlorination of polychlorinated biphenyls on the surface of a Pd/Fe bimetallic system. Environ Sci Technol 1995;29:2898–900.
Han FX, Su Y, Monts DL, Waggoner CA, Plodinec MJ. Binding, distribution, and plant uptake of mercury in a soil from Oak Ridge, Tennessee, USA. Sci Total Environ 2006;368:753–68.
Kim H-J, Saleh NB, Phenrat T, Tilton RD, Lowry GV. Effect of pH and clay on the transportability of surface-modified Fe^0 nanoparticles in saturated sand columns. the proceedings of the ACS 82nd Colloids and Surface Science Symposium, NC State University, Raleigh, NC June 15–18, 2008; 2008.
Kohn T, Livi KJT, Roberts AL, Vikesland PJ. Longevity of granular iron in groundwater treatment processes: corrosion product development. Environ Sci Technol 2005;39:2867–79.

Lee W, Batchelor B. Abiotic reductive dechlorination of chlorinated ethylenes by iron-bearing soil minerals. 1. Pyrite and magnetite. Environ Sci Technol 2002a;36:5147–54.
Lee W, Batchelor B. Abiotic reductive dechlorination of chlorinated ethylenes by iron-bearing soil minerals. 2. Green Rust. Environ Sci Technol 2002b;36:5348–54.
Lien H-L, Zhang W-x. Nanoscale iron particles for complete reduction of chlorinated ethenes. Colloid Surface A 2001;191:97-105.
Liu Y, Lowry GV. Effect of particle age (Fe^0 content) and solution pH on nZVI reactivity: H2 evolution and TCE dechlorination. Environ Sci Technol 2006;40:6085–90.
Liu Y, Majetich SA, Tilton RD, Sholl DS, Lowry GV. TCE dechlorination rates, pathways, and efficiency of nanoscale iron particles with different properties. Environ Sci Technol 2005;39:1338–45.
Matheson LJ, Tratnyek PG. Reductive dehalogenation of chlorinated methanes by iron metal. Environ Sci Technol 1994;28:2045–53.
Nurmi JT, Tratnyek PG, Sarathy V, Baer DR, Amonette JE, Pecher K, Wang C, Linehan JC, Matson DW, Penn RL, Driessen MD. Characterization and properties of metallic iron nanoparticles: spectroscopy, electrochemistry, and kinetics. Environ Sci Technol 2005;39:1221–30.
Orth WS, Gillham RW. Dechlorination of trichloroethene in aqueous solution using Fe^0. Environ Sci Technol 1996;30:66–71.
Phenrat T, Saleh N, Sirk K, Tilton RD, Lowry G. Aggregation and sedimentation of aqueous nanoscale zerovalent iron dispersions. Environ Sci Technol 2007;41:284–90.
Reddy K, Karri MR. Removal and degradation of pentachlorophenol in clayey soil using nanoscale iron particles. Geotechnics of Waste Management and Remediation, Geotechnical Special Publication No.177. Reston, Virginia: ASCE Press; 2008. p. 463–9.
Roberts AL, Totten LA, Arnold WA, Burris DR, Campbell TJ. Reductive elimination of chlorinated ethylenes by zero-valent metals. Environ Sci Technol 1996;30:2654–9.
Staudinger J, Roberts PV. A critical compilation of Henry's law constant temperature dependence relations for organic compounds in dilute aqueous solutions. Chemosphere 2001;44:561–76.
Su C, Puls RW. Kinetics of trichloroethene reduction by zerovalent iron and tin: pretreatment effect, apparent activation energy, and intermediate products. Environ Sci Technol 1999;33:163–8.
US EPA. Workshop on Nanotechnology for Site Remediation, U.S. Department of Commerce Washington, DC; 2005. October 20–21.
Van Genuchten MT, Wierenga PJ. Solute Dispersion Coefficients and Retardation Factors, vol. 9. Soil Science Society of America Book Series; 2003. p. 1025–54. Part 1.
Wang C-B, Zhang W-X. Synthesizing nanoscale iron particles for rapid and complete dechlorination of TCE and PCBs. Environ Sci Technol 1997;31:2154–6.
Watson DB, Kostka JE, Fields MW, Jardine PM. The Oak Ridge Field Research Center Conceptual Model. NABIR report; 2004.
Zhang W-x. Nanoscale iron particles for environmental remediation: an overview. J Nanopart Res 2003;5:323–32.
Zhang W-x, Wang C-B, Lien H-L. Treatment of chlorinated organic contaminants with nanoscale bimetallic particles. Catal Today 1998;40:387–95.